7

Advances of SiO_x and Si/SiO_x Core-Shell Nanowires

Kuan Yew Cheong and Yi Ling Chiew
School of Materials & Mineral Resources Engineering, Engineering Campus, Universiti Sains Malaysia, 14300 Nibong Tebal, Seberang Perai Selatan, Penang, Malaysia

1. Introduction

Nanotechnology can be defined as the design, construction and utilization of functional materials with at least one of the dimension measured is in nano-scale to exploit the new properties and phenomena developed at that scale. These nanomaterials exhibit new and improved physical, chemical and biological properties, phenomena and processes due to the variation of wavelike properties of electrons inside matter as the size of matter is reduced and the electrons are confined.

Nanowires, one of the one-dimensional nanostructures, are wire-like structure that has diameter less than 100 nm. Single crystal nanowires grow along a specific axial direction though their side surfaces may not be well defined. The cross-section of the nanowires may either be round, hexagonal or polyhedron depending on the crystallography of the material (Lieber & Wang, 2007). The length of nanowires can vary from few hundred of nanometers to micrometer and even millimeters.

In this chapter, we review advances of SiO_x nanowires and Si/SiO_x core-shell nanowires. Nanowires, which are one form of one-dimensional nanostructures, have been used as versatile building blocks in the miniaturization of electronic and optoelectronic devices (Li et al., 2005). Various materials have been synthesized in the form of nanowires, such as silicon, germanium, gallium nitride, gallium arsenide, and silicon carbide (Spanier, 2006). Thus, it is important to understand properties, applications and synthesis methods of the nanowires so as to be able to produce nanowires with well-controlled properties and dimensions to be incorporated into electronic devices. Here in this review, properties, applications and how SiO_x nanowires and Si/SiO_x core-shell nanowires are made are discussed in the following sections. Section 2 gives a brief discussion on the SiO_x nanowires. Section 3 discusses the properties that enable SiO_x nanowires to be successfully used in different applications. Section 4 gives a short review on the potential applications of SiO_x nanowires. Section 5 reviews the different methods used to synthesize the nanowires, which also includes their phenomena, techniques and mechanism. Section 6 gives a brief discussion on Si/SiO_x core-shell nanowires. Section 7 discusses the important properties of Si/SiO_x core-shell nanowires that are linked to their potential applications. Section 8 reviews the different methods used to synthesize the core-shell nanowires. Finally, section 9 concludes by a short summary.

Source: Nanowires Science and Technology, Book edited by: Nicoleta Lupu,
ISBN 978-953-7619-89-3, pp. 402, February 2010, INTECH, Croatia, downloaded from SCIYO.COM

2. SiO_x nanowires

Silicon oxide (SiO_x) nanowires have been reported to be amorphous, where there is no long-range order of positions of the atoms (Sood et al., 2006). SiO_x may exist in different ratio of silicon and oxygen. The atomic ratio of silicon and oxygen in SiO_x has the x value between 1 and 2 (Zhang et al., 1999). Different methods had been used to synthesize SiO_x nanowires though the ratio of Si:O differed from one another but they remained in the range of $1 \leq x \leq 2$. Table 1 lists down the values of x of the SiO_x nanowires produced using different methods.

Methods	*References*	*x value in SiO_x*
Laser Ablation	Aharonovich et al. (2008)	1<x<2
Chemical Vapor Deposition	Ni et al. (2006)	2
	Zheng et al. (2002)	2
	Zhang et al. (2006)	1.3
	Jiang et al. (2005)	1.2
	Yang et al. (2007)	1.8 – 2.1
Sol-Gel Processing	Liang et al. (2000)	1.4
Rapid Thermal Annealing	Lai et al. (2008)	1:2
Ion Implantation	Sood et al. (2006)	1<x<2
Carbon-Assisted Growth	Zhu et al. (1998)	1<x<2
	Saulig-Wenger (2003)	2
Thermal Oxidation Route	Hu et al. (2003)	2

Table 1. List of Si:O ratio of the silicon oxide nanowires produced using different methods.

3. Properties of SiO_x nanowires

Since dimensionality alters the properties of a structure as the dimension decreases, it is then important to understand the properties of SiO_x nanostructures so as to enable the exploitation of these materials for new applications. Some of these properties are summarized in the Table 2.

Properties	*Value*
Young's Modulus	57 – 93 GPa
Electrical	Varies according to number of Si-O bonds (changes from metallic to insulating as number of bonds increase)
Fermi level	-3 eV to -7 eV (more positive as number of Si-O chain increases)
PL band energies	1.9 – 4.3 eV

Table 2. Properties of SiO_x nanowires (Wei et al., 2006, Jin et al., 2008, Ni et al., 2006 and Bilalbegović, 2006).

3.1 Optical properties of SiO_x nanowires

Various SiO_2 glasses and nanowires have different photoluminesence (PL) energy peaks ranging from 1.9 to 4.3 eV according to Wei et al. (2006). From the study performed by Jin et

al. (2008), a strong blue–green emission was observed (Figure 1) with the peak centered at 2.5 eV (about 500 nm).

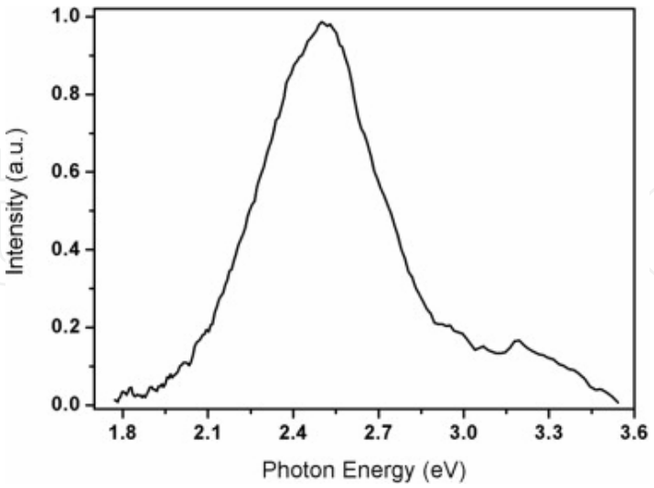

Fig. 1. Room temperature PL spectrum of the as-fabricated nanostructures showing a strong emission peak centered at 2.5 eV (Jin et al., 2008).

Similarly, Wu et al. (2001) reported that a stable and strong blue emission was found at 2.85 eV (435 nm) at room temperature under excitation at 260 nm while ultraviolet and blue light emission at 3.54 eV (350 nm), 3.0 eV (420 nm) and 2.7 eV (465 nm) could also be observed (Figure 2). The different values of energy bands had been attributed to certain phenomenon. The 3.0 eV band (415 nm) could be attributed to two-fold coordinated silicon lone-pair centers (Itoh et al., 1989). The 2.7 eV band (460 nm) was due to neutral oxygen vacancy. These defects are due to oxygen deficiency in the obtained products (Meng et al., 2003). These oxygen deficiencies in the SiO_x nanowires account for the blue-green emission around 500 nm. The 2.2 eV band (566 nm) was due to the self-trapped excitons that were confined to a SiO_4 tetrahedron (Lee et al., 2004). With the decrease of oxygen vacancies, the intensity of the green emissions would increase.

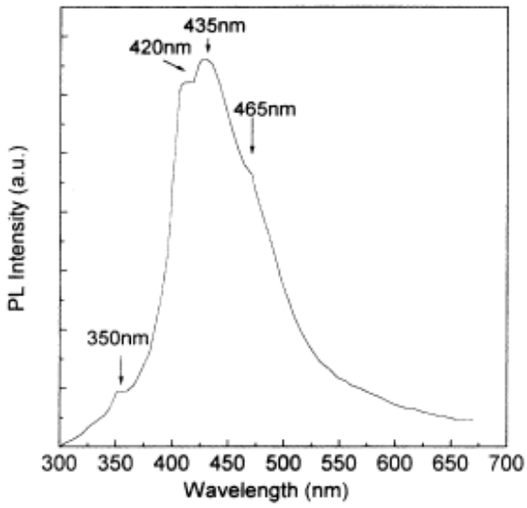

Fig. 2. PL spectrum of SiO_x nanowires under excitation at 260 nm (Wu et al., 2001).

3.2 Elastic modulus of SiO_x nanowires

Measurement of mechanical properties of the SiO_x nanowires is very important since these nanowires can be integrated into functional nanodevices without leading to malfunction or failure of the entire device. This is because the devices are always subjected to some form of mechanical forces during usage. Thus, if the nanowires used to produce the devices have good mechanical properties, then the devices can function effectively. To determine the elastic modulus of the amorphous SiO_x nanowires, nano-scale three-point bending tests can be performed directly on individual amorphous SiO_x nanowires using an atomic force microscope (AFM). Ni and Gao (2006) found that the elastic modulus of the amorphous SiO_2 nanowires was 76.6 ± 7.2 GPa. The amorphous SiO_2 nanowires also exhibited brittle fracture failure in bending.

Based on the assumption that the nanowire follows linear elastic theory of an isotropic material, the elastic modulus of the SiO_2 nanowire, E_n, can be calculated from the following equation (Ni and Gao, 2006).

$$E_n = \frac{FL^3}{192 d_n I} = \frac{k_n L^3}{192 I} \tag{1}$$

where

I is the moment of inertia and for a round-shaped nanowire, $I=\pi r^4/4$,
r is the radius of nanowire,
L is the suspended length of nanowire,
F is the applied load at its midpoint position,
k_n is the spring constant of nanowire ($k_n = F/d_n$).

For all tested nanowires with a diameter ranging from 50 nm to 100 nm, the calculated elastic modulus ranged from 57 to 93 GPa and the average elastic modulus is 76.6 ± 7.2 GPa, which is close to the reported value of 73 GPa of thermally grown SiO_2 thin films and bulk SiO_2, but lower than that of plasma-enhanced CVD (PECVD) SiO_2 thin films (Ni and Gao, 2006). Normally, PECVD SiO_2 thin films usually exhibit a higher elastic modulus than thermally grown ones. It can be seen from Figure 3 that the elastic modulus of the amorphous SiO_2 nanowires was independent of the wire diameter in the range of 50–100 nm.

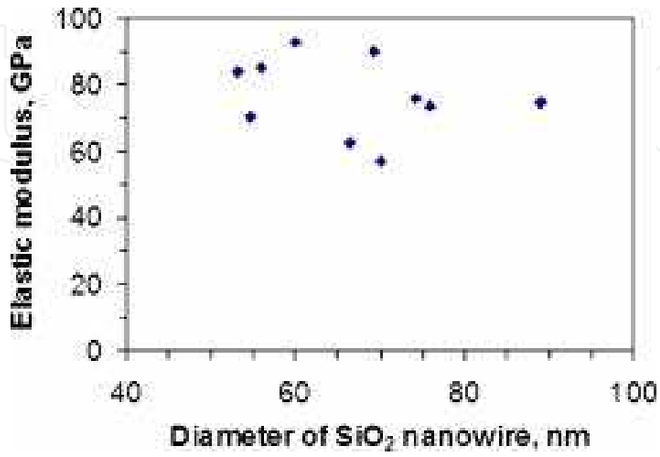

Fig. 3. Bending elastic modulus of the amorphous SiO_2 nanowire vs nanowire diameters (Ni et al., 2006).

3.3 Electronic properties of SiO_x nanowires

To integrate SiO_x nanowires into electronic components, it is important to understand their electronic properties. Bilalbegović (2006) used a computational method to investigate the electronic properties of the different structures of SiO_x nanowires consisting of linear chain, zigzag chain and long Si_4O_8 nanowires. The plot of the electronic structure of a linear, zigzag chain and Si_4O_8 nanowires are shown in Figure 4. The electronic structure of the linear chain in Figure 4(a) showed that one band crossed the Fermi level, and thus the system is metallic. For both zigzag and the long Si_4O_8 nanowires, the wires were insulator since there was no crossing of bands through the Fermi level. This indicated that as the number of neighbors in Si-O nanowires increased or changed from nanoscale to bulk size, the electronic behavior went from metallic to insulating.

The distances between the Si-O and Si-Si bonds in zigzag chains were computed to be smaller than that of linear chains simulated by Bilalbegović (2006). The Si–O distances in the three types of nanowires are larger than in the majority of silica bulk phases. It was due to rearrangement of the atoms that led to compression of bonds, and thereby removed a crossing band from the Fermi level in the zigzag chains and resulted in an insulating behavior in the structure. For the case of linear chains, the weak metallic behavior was due to weaker bonding and small coordination. The existence of a metallic state offered the possibility to use these nanowires in conducting nanodevices without doping.

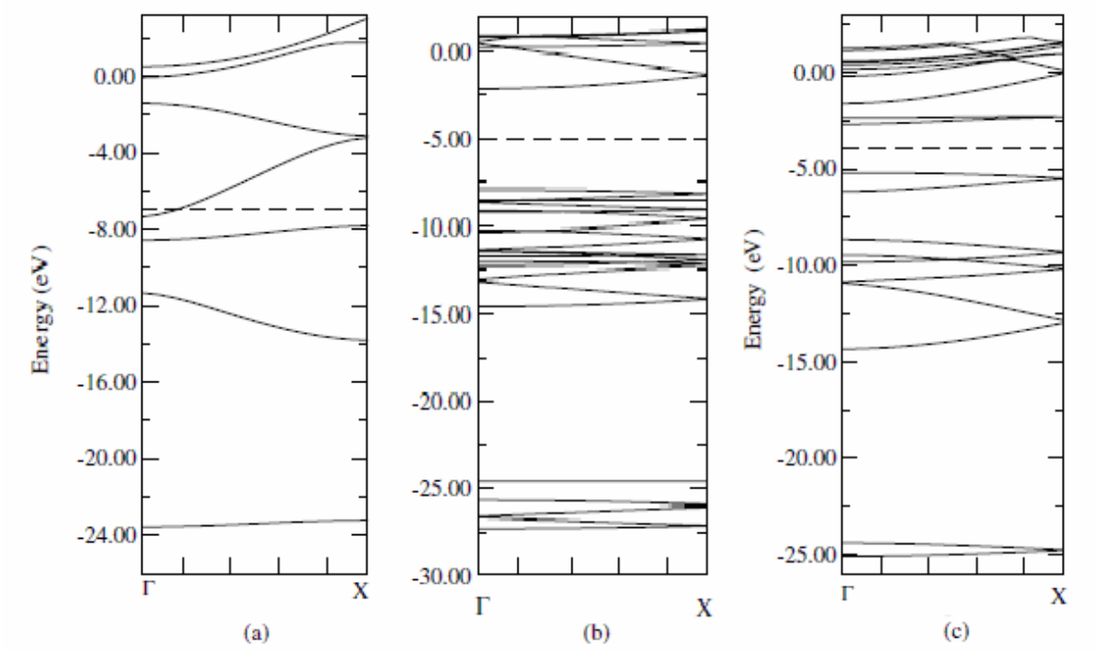

Fig. 4. Energy band structures of a) linear chain, b) zigzag chain and c) Si_4O_8 nanowires where the dashed lines denoted the Fermi levels (Bilalbegović, 2006).

4. Applications of SiO_x nanowires

SiO_x-based nanostructures have gained much interest due to their interesting properties as discussed in the previous section. Their photoluminescence properties in the range of 1.9 to 4.3 eV, emitting blue-green light makes them suitable to be made into photoluminescence

materials such as intensive blue light emitters by Yu et al. (1998), integrated optical nanodevices and high resolution optical heads scanning near-field optical microscope (Cai et al., 2005). Furthermore, they are also being investigated for application as low-loss optical wave guiding (Tong et al., 2003). Their excellent bio-compatibility also makes these nanostructures suitable to be used in biomedical applications. For example, poly-L-lysine modified SiO_2 nanoparticles were developed by Li et al. (2005) as a nonviral vector for gene delivery.

5. Synthesis methods of SiO_x nanowires

The development of SiO_x nanowires have been reported since its discovery by Yu et al. (1998). Basically there are two different fabrication approaches, non-catalyst-based and catalyst-based methods. The non-catalyst-based methods usually involve silicon wafers (Dai et al., 2003), SiO_2 nanoparticles (Fang et al., 2005), or a mixture of Si/SiO_2 powder (Zhang et al., 2000) as source materials with the oxygen from either the oxygen flow, silica powder or residue O_2 gas in the chamber or carrier gas. The temperature involved in these methods is usually very high, reaching temperatures over 1000 ^oC as well as a long growth time. The catalyst-based methods, in the mean time, require a much lower temperature and shorter time. Different kinds of catalysts have been used to induce the growth of SiO_x nanowires such as TiN (Lee et al., 2004), Ga (Dai et al., 2005), In2O3 (Wang et al., 2003), Fe (Lee et al., 2003) and Pt (Lai et al., 2008). These methods are normally associated with vapor-liquid-solid mechanism. In the following sections, the different types of synthesis methods will be discussed briefly.

5.1 Excimer laser ablation

SiO_x or SiO_2 nanowires have been synthesized by this technique (Yu et al., 1998). The typical experiment was carried out by using an excimer laser to ablate the target in an evacuated quartz tube filled with Ar gas. The solid target could be highly pure SiO_2 powder mixed with metals (Fe or Ni). In a study performed by Yu et al. (1998), highly precise form of SiO_x nanowires were obtained by using ablation from an excimer laser to mill the tip of a SiO_2 material. The ablation process had been used to produce nanowires of diameter of 15 nm and hundreds of microns long and emit blue light from optical pumping.

Aharonovich, Tamir and Lifshitz (2008) also used laser ablation to produce SiO_x nanowires. The laser targets were pure Si and mixed Si–5%Au, where the Au is used a catalyst to induce the growth of nanowires. A pulsed neodymium doped yttrium aluminum garnet laser with wavelength of 266 nm was used to ablate the different targets in a heated evacuated tube, with the Au-coated or Ni-coated substrates on which the nanowires were supposed to grow placed along the tube. The products formed are as shown in Figure 5 that showed that the nanowires grown on sapphire substrates using different catalyst and target. The nanowires grown by Bi are longer than those of Au.

5.2 Chemical Vapor Deposition (CVD)

Chemical vapor deposition is a process which involves a chemical change occurring in the vapor phase, whether through rearrangement of the source materials' elements, made possible by excess energy provided to the system, or through reactions of the source vapors with the gasses introduced into the system. This process is normally associated with the vapor-liquid-solid (VLS) growth mechanism (Ni et al., 2006 and Zhang et al., 2006).

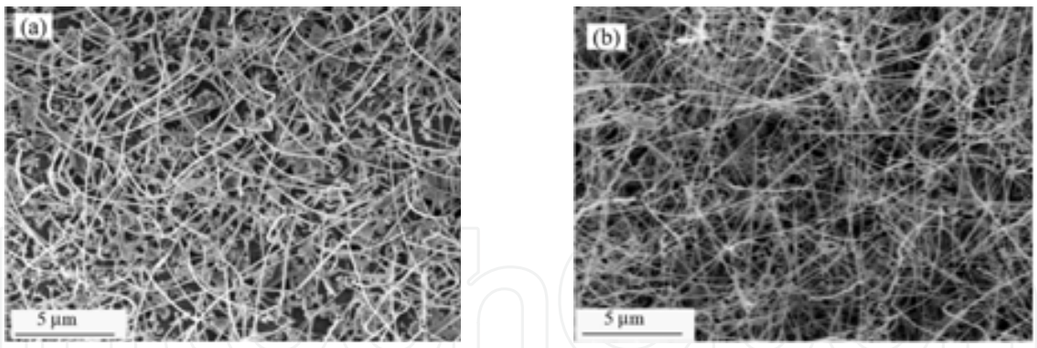

Fig. 5. HRSEM images of SiO_x nanowires on sapphire substrates after growth at (a) 1050 °C with Au catalyst, use of mixed Si–5%Au target and (b) 1150 °C with Ni catalyst, use of Si target (Aharonovich, Tamir and Lifshitz, 2008).

This mechanism was proposed by Wagner and Ellis in 1964 for silicon whisker growth and has been widely used to guide the growth of various kinds of one-dimensional nanostructures. This mechanism first involves the formation of a liquid eutectic alloy droplet composed of metal catalyst component such as Au and Ga under the reaction conditions that serves as a preferential site for nucleation site for crystallization and growth. During growth, the catalyst droplet alloy directs the growth direction of nanowires and defines the diameter of the crystalline nanowire. The nanowire stops growing when the temperature drops below the eutectic temperature of the catalyst alloy or the reactant is not available anymore. As a result, the nanowires obtained through this mechanism typically have a solid catalyst nanoparticle with diameter comparable to that of the connected nanowire.

Jiang et al. (2005) have reported the synthesis of SiO_2 nanowires and nanotubes through a simple CVD system using alumina wafers and silicon powder with Fe-Co-Ni alloy nanoparticles as catalyst. The nanowires formed had diameters of around 100 nm and length up to 100 μm. The nanowires formed had nanoparticles attached at each end of the nanowires [Figure 6(a)], which is a characteristic of product formed from the VLS growth mechanism and CVD.

Another study performed by Yang et al. (2007) using CVD produced amorphous SiO_2 nanowires of diameter 30 – 80 nm and length of several tens of micrometers. The source material used was pre-oxidized substrates catalyzed by Ni-based catalyst under ambient

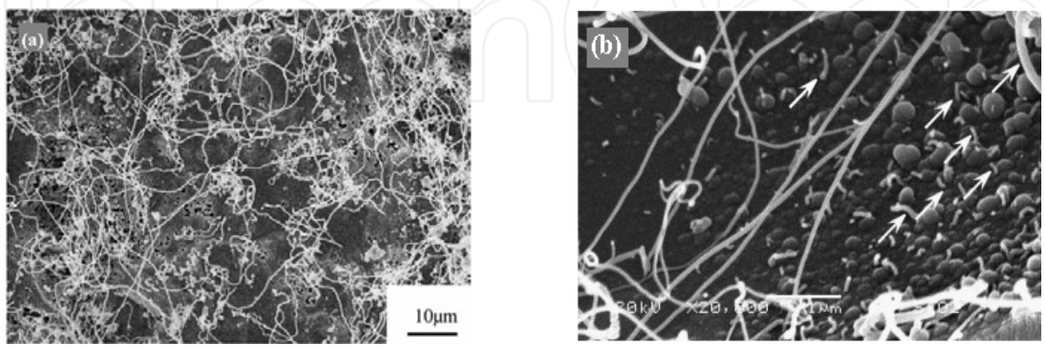

Fig. 6. SEM image of silica nanowires a) grown on alumina substrate (Jiang et al., 2005) and b) grown on pre-oxidised silicon substrate with some catalyst particles as indicated by the arrows (Yang et al., 2007).

pressure. Some catalyst particles were also observed on the SiO_2 nanowires [Figure 6(b)]. The growth was found to be non-uniform due to non-uniform decomposition of the catalyst $Ni(NO_3)_2$.

5.3 Sol-Gel template

SiO_2 nanowires can also be produced by this method. According to the study by Liang et al. (2000), mesoporous SiO_2 xerogel containing Fe nanoparticles, prepared by a sol–gel process from tetraethoxysilane (TEOS) hydrolysis in iron nitrate aqueous solution, was crushed into powder and mixed with silicon powder ground from a single crystal silicon plate with a molar ratio of SiO_2 to Si being slightly greater than 1. The source materials were then heated in a flowing Ar atmosphere. Most of the nanowires formed were straight and smoothly curved [Figure 7(a) and (b)], while others are helical-like [Figure 7(c)] or braided-like wires [Figure 7(d)]. The diameters of the braided and helical-like nanowires were about 10–25 nm, which were smaller than those of the straight and smoothly curved nanowires of about 40–50 nm. The lengths of all these nanowires were up to several tens of micrometers.

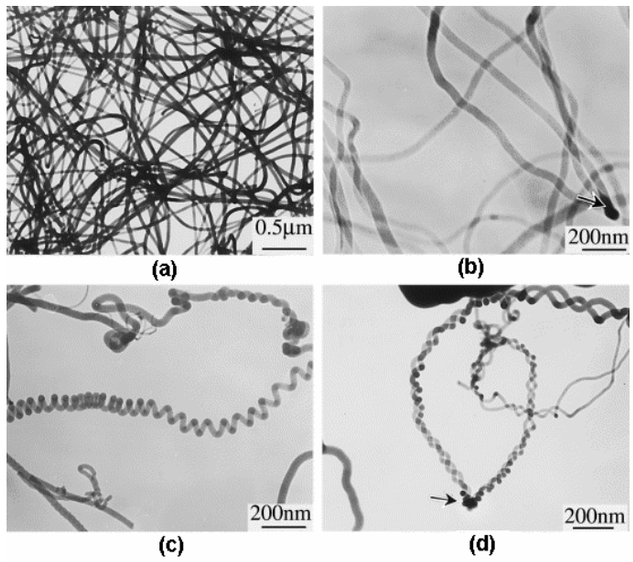

Fig. 7. TEM images of (a) straight, (b) smoothly curved, (c) helical-like and (d) braided-like SiO nanowires (Liang et al., 2000).

Zhang et al. (1999) also use a sol-gel method to prepare aligned SiO_x nanostructures on an anodic alumina as shown in Figure 8. The SiO_2 sol was prepared from mixing of TEOS solution, HCl and ethanol at room temperature and was left to age for several days at room temperature. The highly ordered nanochannel-array of anodic alumina was then dipped into the sol, removed to dried and finally heated in air at 200 ^oC for two day.

5.4 Rapid thermal annealing (RTA)

RTA refers to a semiconductor manufacturing process which heats the substrates to high temperatures (up to 1200 ^oC or greater) in a short time of several seconds but this rate does not apply to cooling. Slow cooling is performed to avoid the failure of substrates due to thermal shock. In addition, the soak time for RTA is much shorter than that for a furnace. These processes are used for a wide variety of applications in semiconductor manufacturing

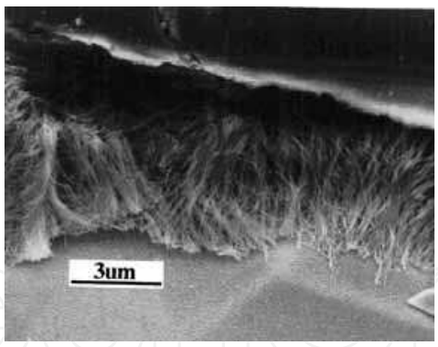

Fig. 8. SEM image of silicon oxide nanowires obtained by immersing the anodic alumina in the sol which is aged at room temperature for 2 days (Zhang et al., 1999).

including dopant activation, thermal oxidation, metal reflow and synthesis of nanostructures (Nishi & Doering, 2000).

Lai et al. (2008) used RTA to synthesize SiO_x nanowires on a Pt-coated pre-oxidized p-type silicon (100) substrates. The oxide layer thickness was 11 nm whereas the Pt layer ranged from 15, 30 and 50 nm. The $Pt/SiO_2/Si$ structure was subjected to RTA in nitrogen atmosphere at 900 ^oC for 60 s. No nanowires were observed at the annealing temperature of 800 ^oC since the growth temperature of the SiO2 nanowires is above the Pt-Si eutectic temperature of 847 ^oC. Nanoparticles of Pt were found at the tip of the nanowires as shown in Figure 9, corresponding to the VLS growth mechanism. The diameter of the nanowires ranges from 30 nm to 150 nm with length up to 1 μm. The diameter was believed to be related to the size of the seed particles.

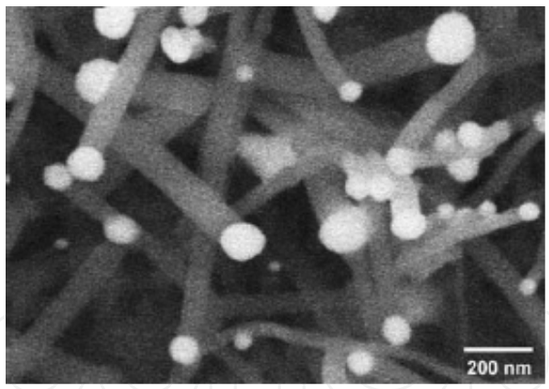

Fig. 9. SEM image of Pt-assisted SiO_2 nanowires grown after rapid thermal annealing at 900°C for 60 s (Lai et al., 2008).

5.5 Ion implantation

Ion implantation is a process in which ions of a material are implanted into another solid. The ions cause a change in the physical properties of the solid as well as in the chemical properties of the solid since the ions can be of different element than the solid (Nishi & Doering, 2000).

In the case of producing SiO_x nanowires using ion implantation as performed by Sood et al. (2006), Pd ions were first implanted on the prime grade Si (100) wafers in certain regions using an Al shadow mask. The ion dose varied from 5×10^{12} to 3×10^6 Pd ions/cm^2. The

ion-implanted wafers were then annealed at 1100 ^{o}C in argon ambient to grow the nanowires. The nanowires grown had diameters ranging from about 15 to 90 nm with length varied up to about 50 μm. It was also found that the nanowires' size and distribution could be controlled by varying the ion dose, as shown in Figure 10. It was found that an ion dose of about 10^{16} ions/cm^2 was required to produce the nanowires.

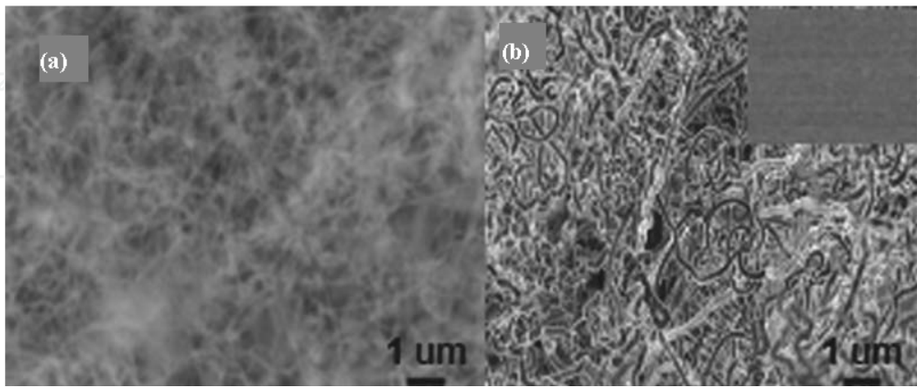

Fig. 10. Effect of implanted dose on the growth of SiO_2 nanowires heated at 1100 °C for 60 min where. (a) 3 x 10^{16} ions/cm^2—high density thinner nanowires and (b) 1 x 10^{16} ions/cm^2—thicker coiled nanowires of reduced density. Inset: 5 x 10^{12} ions/cm^2—absence of nanowires (Sood et al., 2006).

5.6 Carbon assisted growth

Carbon assisted growth is a process in which carbon plays an important role. Carbon can assist the growth of SiO_x nanowires but the opinions on the nanowire formation mechanism differ from one report to another report (Li et al., 2004). From information obtained from the Li et al. (2004), it was found that CO or CO_2 component played an important role in the synthesis of SiO_x nanowires depending on the setup used.

Saulig-Wenger et al. (2003) have reported the synthesis of amorphous SiO_2 nanowires with only silicon powder in the presence of graphite in a furnace without any catalyst. The SiO_2 nanowires had lengths up to 500 mm for diameters in the range of 10–300 nm as shown in Figure 11. The Ar : O_2 carrier gas ratio was 99.2 mol% : 0.8 mol%, and the growth

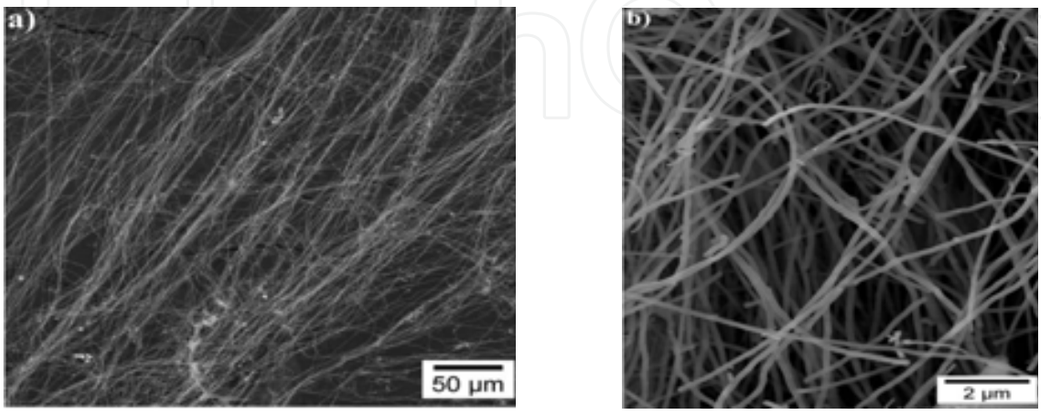

Fig. 11. SEM images of the SiO_2 nanowires formed through carbon-assisted growth (Saulig-Wenger et al., 2003).

temperature was 1200 °C. They found the relative O_2 flow rate played a very important role in the formation of the nanowires. Based on their study, it was found that having either no O_2 or a large amount of O_2 hindered the nanowire growth and that CO_2, not CO was the decisive factor in the growth of nanowires.

Li et al. (2004) also used carbon-assisted growth to synthesize SiO_x nanowires with a short growth time (30 min) on Au-coated silicon substrates. The formation of the SiO_x nanowires depends on the experimental conditions, such as substrate coating (Au), the presence of graphite powder, the substrate temperature, the oxygen flow, and the growth time. The optimum growth conditions in this study are a substrate temperature of 1000 °C, an Ar flow of 250 sccm, and an O_2 flow of 5 sccm. It was also demonstrated that the formation of the SiO_x nanowires was due to a solid-liquid-solid (SLS) mechanism, and the locally catalytic oxidation of CO by Au nanoclusters may play a role in accelerating nanowire formation.

6. Si/SiO_x core-shell nanowires

SiO_x nanowires sometimes also form a core-shell structure with the crystalline core and amorphous shell. From previous studies, the core can be either the combination of Ga, Ni, Si and O (Cai et al., 2005), Ge (Arnold et al., 2009), SiC (Liu and Yao, 2005) and Si (Jia et al. 2007, Pan et al., 2001, Kolb et al., 2004, King et al., 2008, Park and Yong, 2004, Yao et al., 2005). There was also report on SiO_x/ZnO core-shell nanowires, where the core consisted of amorphous SiO_x while the shell consisted of crystalline ZnO (Kim et al., 2007). Here, we will only focus on Si/SiO_x core-shell nanowires whereby the core consisted of crystalline silicon and the shell of amorphous SiO_x. Silicon nanowires can also be obtained by etching the silicon oxide off the core-shell nanowires using HF solution. The applications of Si/SiO_x core-shell nanowires are similar to those of silicon nanowires.

7. Properties of Si/SiO_x core-shell nanowire

The properties of these core-shell structures are similar to those of silicon nanowires. The amorphous shell helps to prevent the mechanical or radiation damage and suppress chemical reactivity, which could lead to oxidation and contamination in the silicon nanowire. However, there are only a few studies that report on the properties on the core-shell nanowires (Jia et al., 2007, King et al., 2008). Below is compilation of the properties being reported.

7.1 Optical properties of Si/SiO_x core-shell nanowires

Research has been carried out on the origin of light emission in the nanowires. Several origins have been proposed, including the existence of excess silicon atoms in the silicon nanostructure, defect centers in the SiO_x layer that surrounds the nanowires defects in the SiO_x and the interface between the SiO_x and nanoparticles in the case of chainlike nanowires incorporating crystalline silicon spheres (King et al., 2008). The Si/SiO_2 core-shell nanowires formed had different morphologies ranging from chain-like structure [Figure 12(a)], tadpole-like structure [Figure 12(b)] and straight core-shell nanowires [Figure 12(c) and (d)], with each synthesized using different methods. The chain-like structure and tadpole-like structure were produced using oxide-assisted growth while the straight core-shell nanowires were produced using thermal evaporation and CVD. PL occurred across the

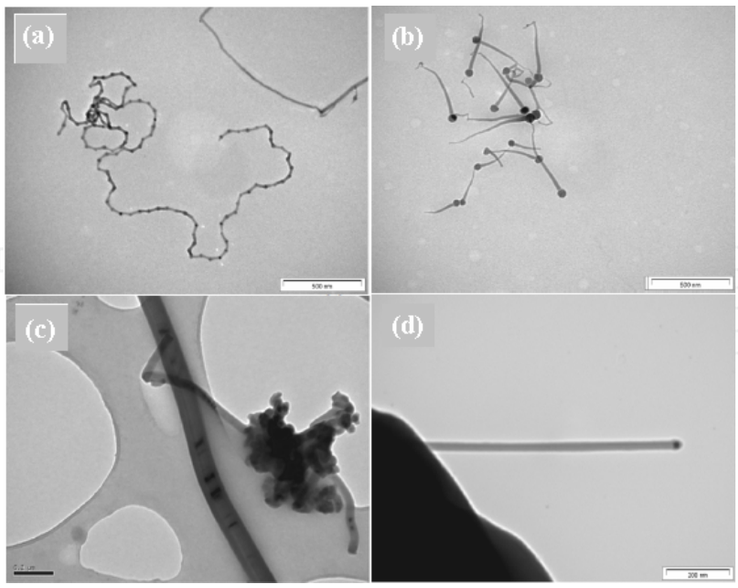

Fig. 12. TEM study of nanostructures: (a) Chain-like structure of crystalline silicon spheres encapsulated by silicon oxide, (b) Tadpole-like structure containing crystalline silicon spheres encapsulated by silicon oxide, (c) Straight nanowires of crystalline silicon encapsulated by SiO_x produced using thermal evaporation and (d) Straight nanowires of crystalline silicon nanowires encapsulated by SiO_x produced using CVD (King et al., 2008).

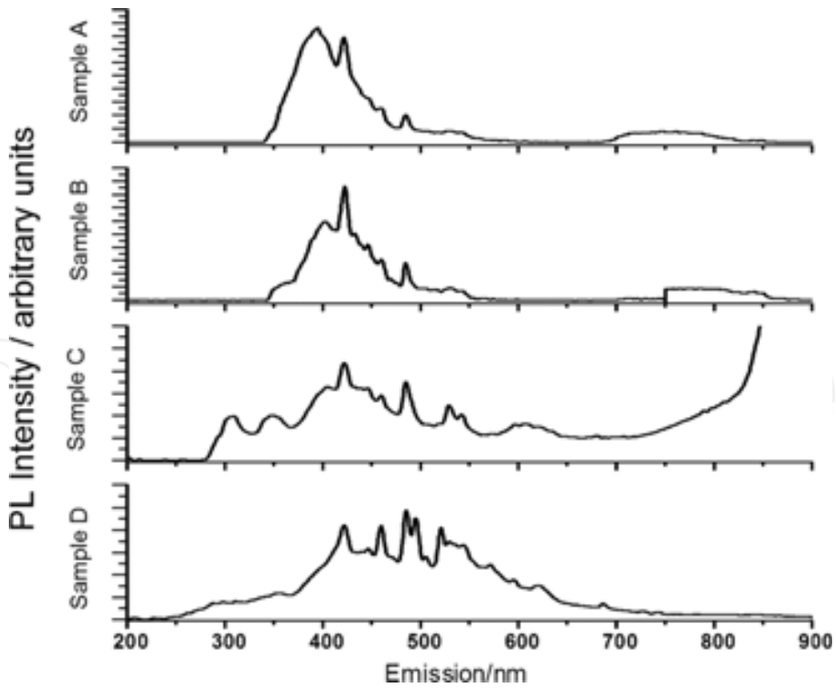

Fig. 13. PL spectrum of each sample when excited at 200 nm (King et al., 2008).

visible region for all the samples. PL in the red region (700 – 800 nm) was due to the radiative recombination of carriers in silicon nanocrystallites formed at the Si/SiO_x interface

(Figure 13). The radiative decay of self trapped excitons at the Si/SiO_x interface resulted in the PL characteristics in the yellow region, which is the main emission in the region for the straight core-shell nanowires, whereas for both chain-like and tadpole-like structures, the main emission region occurred in the ultra-violet to violet region (350 – 450 nm), which was attributed to the direct recombination of carriers at the interface of crystalline silicon nanoclusters and oxide shell.

A study from Jia et al. (2007) on the cathodoluminescence (CL) properties of Si/SiO_x core-shell nanowires showed three main bands at 77 K for all samples [Figure 14(a)], with their maxima at about 620 – 650 nm with wavelength of 2.0 – 1.91 eV (peak 1), 920 nm with wavelength of 1.35 eV (peak 2) and 1270 nm with wavelength of 0.97 eV (peak 3) as well as a shoulder at about 500 nm (peak 0). At room temperature as shown in Figure 14(b), an additional peak around 1570 nm of wavelength 0.79 eV was observed. Peak 1 was attributed to the oxygen deficient centers (ODCs) in the silicon oxide matrix. Peak 2, which was the second order diffraction of peak 0, was attributed to the band-band recombination of crystalline silicon bulk materials and the crystalline core of the silicon nanowires. Peak 3, which was the second order diffraction of peak 1, was attributed to the G-centers near certain twin boundaries. The additional peak at higher temperatures, peak 4 was attributed to the disruption of the efficiency of the recombination channels due to confinement of excess carriers in the silicon nanowires. Infrared emission was also reported at around 1550 nm due to high density of extended defects and oxygen accommodation within the extended defects.

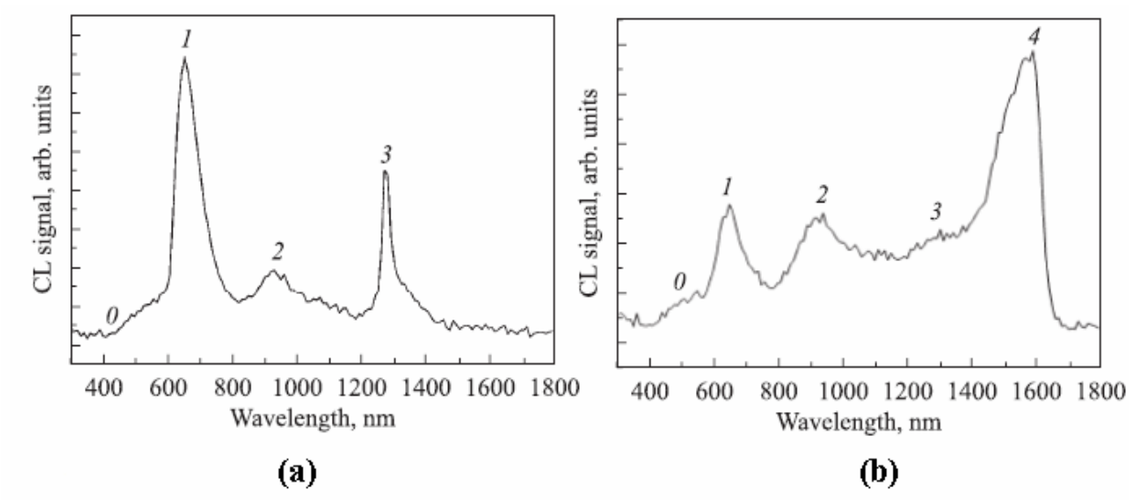

Fig. 14. CL spectrum at (a) liquid nitrogen temperature and (b) at room temperature (Jia et al., 2007).

7.2 Absorption characteristics of Si/SiO_x core-shell nanowires

An understanding of the absorption characteristics of the nanowires will allow the researchers to determine the quantum confinement effects of nanowires. Quantum confinement is said to correspond to the red-shift Γ25 – Γ15 (3.4 eV) direct transition. King et al. (2008) had performed the absorption test besides the PL test. The four samples, chain-like structure [Figure 12(a)], tadpole-like structure [Figure 12(b)], straight Si/SiO_x core-shell

nanowires [Figure 12(c) and (d)] showed different absorption spectrum (Figure 15). Both chain-like structure and tadpole-like structure exhibited a strong increase in the absorption above the X4 – X1 (4.3 eV) direct transition. The straight core-shell nanowires produced using thermal evaporation exhibited a broad shoulder in the X4 – X1 and a weak absorption compared to that in the Γ25 – Γ15 region while the straight core-shell nanowires produced using CVD exhibited an absorption shoulder at 3.8 eV and a strong absorption at 4.3 eV. The quantum confinement phenomenon could only be observed when the nanowires contained crystalline cores due to nucleation kinetics at the Si/SiO_x interface.

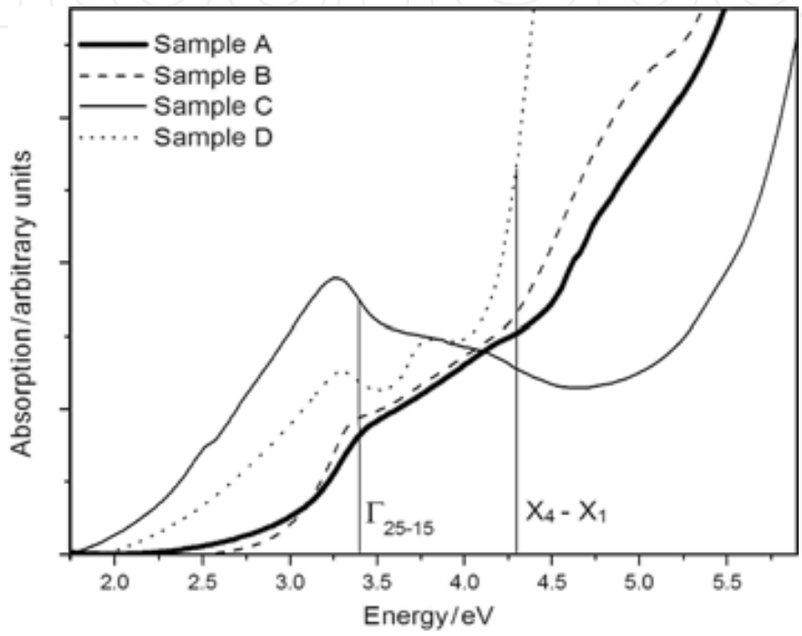

Fig. 15. Optical absorption spectrum of nanowires of different morphologies (King et al. 2008).

8. Synthesis methods of Si/SiO_x core-shell nanowires

Si/SiO_x core-shell nanowires have been synthesized as by-products in the process of obtaining Si nanowires through different methods such as oxide-assisted growth (King et al., 2008, Park & Yong, 2004, Yao, Li & Lee, 2005) and thermal evaporation of silicon monoxide (Jia et al. 2007, Pan et al., 2001, Kolb et al., 2004).

8.1 Oxide-Assisted Growth (OAG)

Oxide-Assisted Growth was first proposed by Zhang et al. (2000) to synthesize these core-shell nanowires in the absence of metal catalyst by laser ablating a mixture of Si and SiO_2 powder. The vapor phase Si_yO generated was the main component in the oxide-assisted process. The formation of the nanowires was believed to occur through two steps:

$$Si_yO \rightarrow Si_{y-1} + SiO, y > 1 \quad (2)$$

$$2SiO \rightarrow Si + SiO_2 \quad (3)$$

It was suggested that these decomposition reactions first led to precipitation of Si/SiO_x core-shell nanoparticles. Some of these particles might be piled up and served as seeds for the growth of nanowires in the following steps. Si_yO (y>1) layer at the tip of each nanowire seemed to have a catalytic effect. This layer might be in or near a molten state and thus capable of enhancing atomic absorption, diffusion and deposition. The SiO_2 component in the shell might help to retard the lateral growth of each nanowire. The precipitation, nucleation and growth of Si nanowires always occurred in the region closest to the cold region indicating that the temperature gradient was the driving force for the nanowire growth (Li et al., 2002, Lee, Wang & Lee, 2000). A TEM image of the core-shell nanowires formed through oxide-assisted growth using zeolite and SiO as starting materials by Li et al. (2002) is as shown in Figure 16. The SiO nanoclusters deposited onto the surface of zeolites and disproportionated to form Si and SiO_2 similar to the reactions as explained above.

The OAG method can also be used to synthesize the core-shell nanowires in the presence of Au catalyst. This route was found to have better dimensional control on the nanowires and required a lower growth temperature. Yao et al. (2005), using Au catalyst, successfully produced oriented Si/SiO_x core-shell nanowires through this fabrication route. This route is just the combination of the VLS and OAG methods. The reduced growth temperature relative to that of catalyst-free OAG might be due to the Au catalytic effect in lowering the SiO decomposition temperature. The Au-SiO approach offered some advantages over VLS growth and OAG, such as the absence of toxic and flammable gases and the control of size and epitaxial growth of silicon nanowires. The nanowires generally grow along the [112] and [110] directions, similar to those grown by catalyst-free OAG method and the product in Figure 17.

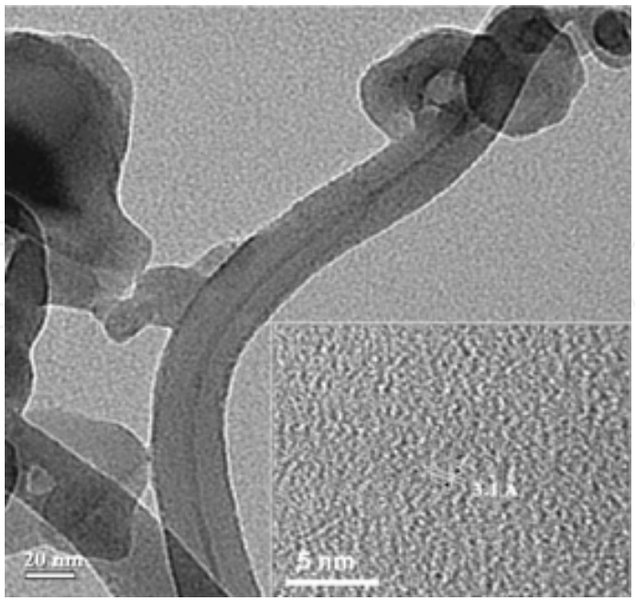

Fig. 16. TEM image of a Si/SiO_2 core-shell nanowires and the inset showed HRTEM image of the same silicon nanowire (Li et al., 2002).

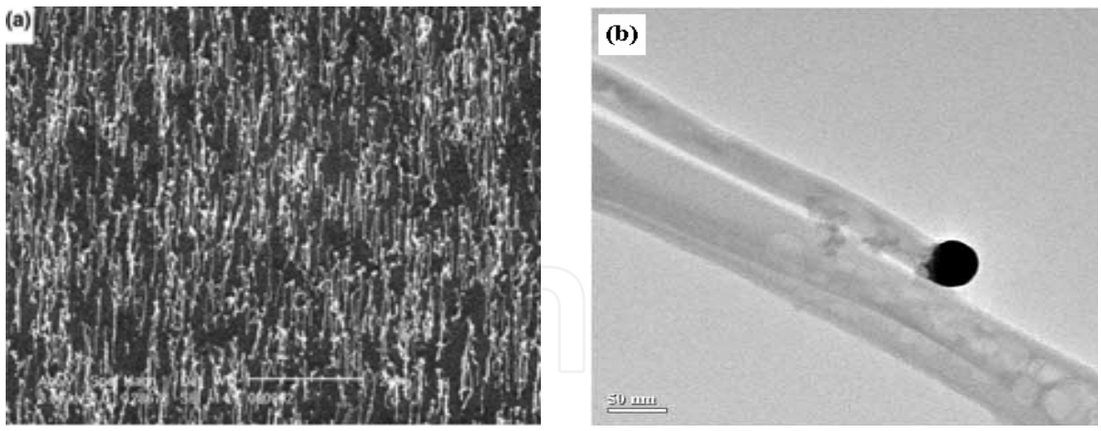

Fig. 17. (a) SEM image of oriented Si/SiO_x core-shell nanowires synthesized at 800 °C and (b) TEM image of a nanowire with a metal particle at the tip (Yao, Li and Lee, 2005).

8.2 Thermal evaporation of SiO powder

Thermal evaporation of SiO powder is a process in which the oxides were found to play an important role in the nucleation and growth of nanowires (Niu et al, 2004, Pan et al., 2001, and Zhang et al., 2000). During annealing, SiO evaporates and transported by the carrier gas to the lower-temperature region to decompose on substrates. It was found that the morphologies of the nanostructures differed as the distance from the SiO source increased when the SiO was transported to lower-temperature region as shown in Figure 18 in a study by Pan et al. (2001). The reaction involved in thermal evaporation of SiO is as follow:

$$2SiO \rightarrow Si + SiO_2 \tag{4}$$

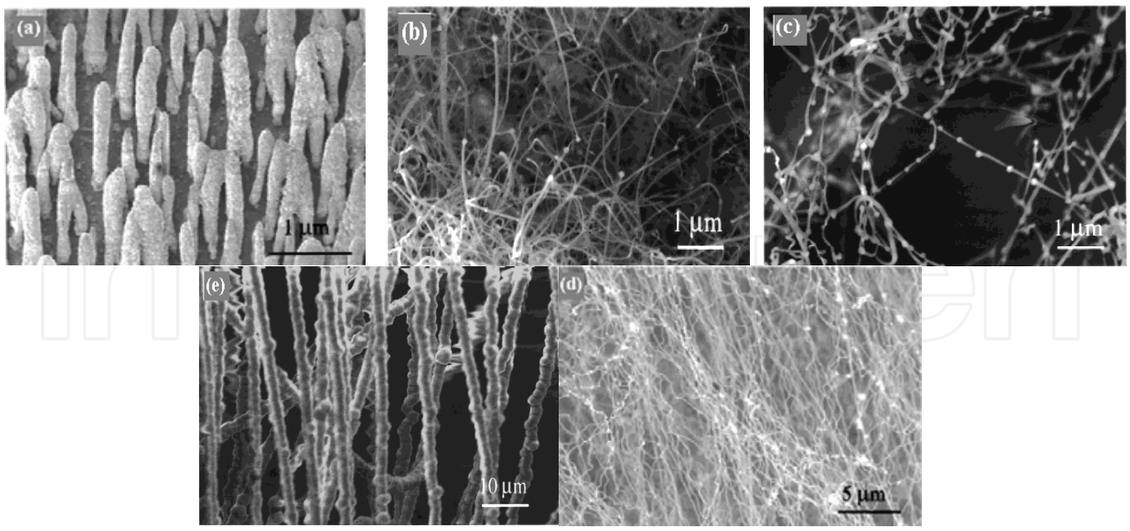

Fig. 18. SEM images of Si/SiO_x core-shell nanowires formed as distance increased from the silicon source (a) Aligned round-tip rods in Zone 1, (b) Yellow circular hard shell of numerous pin-like nanowires in Zone 2, (c) Very fine pinlike nanowires in Zone 3, (d) Si nanowires, which grow along the flowing direction of the carrier gas and form quasi-aligned structures in Zone 4 and (e) Amorphous SiO wires in Zone 5 (Pan et al., 2001).

When the silicon atoms precipitate, the atoms centralize to form the nuclei on some locations on the substrate at which the energy is low such as defects. As the silicon atoms increase, the nuclei will grow up into wires. In this growth route, some of the growth directions of the nanowires will be limited to <111> and <112> orientations due to oxide reaction and growth energy (Niu et al., 2004, Pan et al., 2001).

9. Conclusion

In this review, we have introduced SiO_x nanowires and Si/SiO_x core-shell nanowires. Nanowires have achieved recognition within a very short period of time. The properties of SiO_x and Si/SiO_x core-shell nanowires were reviewed and linked to their relevant applications. Wide range of synthesis methods used to produce the nanowires have also been presented. The nanowires have excellent photoluminescence and mechanical properties as well as biocompatibility, making them potential in the fields of nano-optoelectronics and nono-biotechnology.

10. Acknowledgements

This work was supported by Research University Grant provided by Universiti Sains Malaysia.

11. References

Aharonovich, I., Tamir, S. and Lifshitz, Y., (2008). Growth of SiO_x nanowires by laser ablation, *Nanotechnology*, Vol., 19, 065608 (8 pp), 0957-4484.

Arnold, D.C., Hobbs, R.G., Zirngast, M., Marschner, C., Hill, J.J., Ziegler, K.J., Morris, M.A. and Holmes, J.D., (2009). Single step synthesis of Ge-SiO_x core-shell heterostructured nanowires, *Journal of Materials Chemistry*, Vol., 19, 954-961, 0959-9428.

Bilalbegović, G., (2006). Electronic properties of silica nanowires, *Journal of Physics: Condensed Matter*, Vol., 18, 3829-3836, 0953-8984.

Cai, X.M., Djurišić, A.B. and Xie, M.H., (2005). Growth of SiO_x nanowires, *Proceedings of 2005 5th IEEE Conference on Nanotechnology*, Nagoya, Japan.

Dai, L., Chen, X.L., Jian, J.K., Wang, W.J., Zhou, T. and Hu, B.Q., (2003). Strong blue photoluminescence from aligned silica nanofibers, *Applied Physics A: Materials Science and Processing*, Vol., 76, 625-627, 0947-8396.

Dai, L., You, L.P., Duan, X.F., Lian, W.C. and Qin, G.G., (2005). Growth of silica nanowire arrays by reaction of Si substrate with oxygen using Ga as catalyst, *Physics Letters A*, Vol., 335, 304-309, 0375-9601.

Fang, X.S., Ye, C.H. Xie, T., He, G., Wang, Y.H. and Zhang, L.D., (2005). Synthesis and characterization of ultra-long silica nanowires, *Applied Physics A: Materials Science and Processing*, Vol., 80, 423-425, 0947-8396.

Itoh, C., Suzuki, T. and Itoh, N., (1989). Luminescence and defect formation in undensified and densified amorphous SiO_2, *Physical Review B*, Vol., 41, 3794-3799, 1098-0121.

Jia, G., Arguirov, T., Kittler, M., Su, Z., Yang, D. and Sha, J., (2007). Cathodoluminescence investigation of silicon nanowires fabricated by thermal evaporation of SiO, *Semiconductors*, Vol., 41, No. 4, 391-394, 1063-7826.

Jiang, Z., Xie, T., Yuan, X.Y., Geng, B.Y., Wu, G.S., Wang, G.Z., Meng, G.W., and Zhang, L.D., (2005). Catalytic synthesis and PL of silicon oxide nanowires and nanotubes, *Applied Physics A: Materials Science and Processing*, Vol., 81, 477-479, 0947-8396.

Jin, L., Wang, J.B., Cao, G.Y. and Choy, W.C.H., (2008). Fabrication and characterization of amorphous silica nanostructures, *Physics Letters A*, Vol., 372, Issue 25, 4622-4626, 0375-9601.

Kim, H.W., Shim, S.H., Lee, J.W., Lee, C.M. and Jeoung, S.C., (2008). ZnO-sheathed SiO_x nanowires: Annealing effect, *Optical Materials*, Vol., 30, Issue 7, 1221-1224, 0925-3467.

King, S.M, Chaure, S., Krishnamurthy, S., Blau, W.J., Colli, A. and Ferrari, A.C., (2008). Optical characterization of oxide encapsulated silicon nanowires of various morphologies, *Journal of Nanoscience and Nanotechnology*, Vol., 8, 4204-4206, 1533-4880.

Kolb, F.M., Hofmeister, H., Scholz, R., Zacharias, M., Gösele, U., Ma, D.D. and Lee, S.T., (2004). Analysis of silicon nanowires grown by combining SiO evaporation with the VLS mechanism, *Journal of the Electrochemical Society*, Vol., 151. No. 7, G472-G475, 0013-4651.

Lai, Y.S., Wang, J.L., Liou, S.C. and Tu, C.H., (2008). Tailoring of amorphous SiO_x nanowires grown by rapid thermal annealing, *Chemical Physics Letters*, Vol., 453, Issue 1-3, 97-100, 0009-2614.

Lee, K.H., Lee, S.W., Vanfleet, R.R. and Sigmund, W., (2003). Amorphous silica nanowires grown by the VS mechanism, *Chemical Physics Letters*, Vol., 376, 498-503, 0009-2614.

Lee, K.H., Loftona, C., Kim, K.H., Seo, W.S., Lee, Y.H., Lee, M.H. and Sigmund, W., (2004). Photoluminescence from amorphous silica nanowires synthesized using TiN/Ni/SiO_2/Si and TiN/Ni/Si substrates, *Solid State Communications*, Vol., 131, 687-692.

Lee, S.T., Wang, N. and Lee, C.S., (2000). Semiconductor nanowires:synthesis, structure and properties, *Materials Science and Engineering A*, Vol., 286, Issue 1, 16-23.

Li, C.P., Sun, X.H., Wong, N.B., Lee, C.S., Lee, S.T. and Teo, B.K., (2002). Ultrafine and uniform silicon nanowires grown with zeolites, *Chemical Physics Letters*, Vol., 365, 22-26, 0009-2614.

Li, S.H., Zhu, X.F. and Zhao, Y.P. (2004). Carbon-assisted growth of SiO_x nanowires, *Journal of Physics Chemistry B*, Vol., 108, 17032-17041.

Li, Z., Zhu, S.G., Gan, K., Zhang, Q.H., Zeng, Z.Y., Zhou, Y.H., Liu, H.Y., Xiong, W., Li, X.L. and Li, G.Y., (2005). Poly-L-lysine-Modified Silica Nanoparticles: A Potential Oral Gene Delivery System, *Journal of Nanoscience and Nanotechnology*, Vol., 5, No. 8, 1199-1203.

Liang, C.H., Zhang, L.D., Meng, G.W., Wang, Y.W. and Chu, Z.Q., (2000). Preparation and characterization of amorphous SiO_x nanowires, *Journal of Non-Crystalline Solids*, Vol., 277, Issue 1, 63-67, 0022-3093.

Lieber, C.M. and Wang, Z.L., (2007). Functional Nanowires, *MRS Bulletin*, Vol., 32, 0883-7694.

Liu, X.M. and Yao, K.F., (2005). Large –scale synthesis and photoluminescence properties of SiC/SiO_x nanocables, *Nanotechnology*, Vol., 16, 2932-2935, 0957-4484.

Meng, G.W., Peng, X.S. Wang, Y.W., Wang, C.Z., Wang, X.F. and Zhang, L.D., (2003). Synthesis and photoluminescence of aligned SiO_x nanowire arrays, *Applied Physics A: Materials Science & Processing*, Vol., 76, No. 1, 119-121.

Ni, H., Li, X.D. and Gao, H.S., (2006). Elastic modulus of amorphous SiO_2 nanowires, *Applied Physics Letter*, Vol., 88, 043108, 0003-6951.

Nishi, Y. and Doering, R., (2000). *Handbook of semiconductor manufacturing technology*, CRC Press.

Niu, J.J., Sha, J. and Yang, D., (2004). Silicon nanowires fabricated by thermal evaporation of silicon monoxide, *Physica E: Low-dimensional Systems and Nanostructures*, Vol., 23, Issues 1 - 2, 131-134, 1386-9477.

Pan, Z.W., Dai, Z.R., Xu, L., Lee, S.T. and Wang, Z.L., (2001). Temperature-controlled growth of silicon-based nanostructures by thermal evaporation of SiO powders, *Journal of Physical Chemistry B*, Vol., 105, 2507-2514, 1520-6106.

Park, B.T. and Yong, K.J., (2004). Controlled growth of core-shell $Si-SiO_x$ and amorphous SiO_2 nanowires directly from NiO/Si, *Nanotechnology*, Vol., 15, S365-S370, 0957-4484.

Saulig-Wenger, K., Cornu, D., Chassagneux, F., Epicier, T. and Miele, P., (2003). Direct synthesis of amorphous silicon dioxide nanowires and helical self-assembled nanostructures derived therefrom, *Journal of Materials Chemistry*, Vol., 13, 3058-3061, 1520-6106.

Sood, D.K., Sekhar, P.K. and Bhansali, S., (2006). Ion implantation based selective synthesis of SiO_2 nanowires on silicon wafers, *Applied Physics Letters*, Vol., 88, 143110, 0003-6951.

Spanier, J.E., (2006). One-dimensional semiconductors and oxide nanostructures, In: *Nanomaterials Handbook*, 1st edition Yuri Gogotsi, CRS Press, Taylor & Francis Group, United States of America.

Tong, L.M., Gattass, R.R., Ashcom, J.B., He, S.L., Lou, J.Y., Shen, M.Y., Maxwell, I. and Mazur, E., (2003). Subwavelength-diameter silica wires for low-loss optical wave guiding, *Nature*, Vol., 426, 816-819, 0028-0836.

Wang, J.C., Zhan, C.Z. and Li, F.G., (2003). The synthesis of silica nanowire arrays, *Solid State Communications*, Vol., 125, 629-631, 0038-1098.

Wei, Q., Meng, G.W., An, X.H., Hao, Y.F. and Zhang, L.D., (2006). Synthesis and photoluminescence of aligned straight silica nanowires on silicon substrate, *Solid State Communications*, Vol., 138, Issue 7, 325-330, 0038-1098.

Wu, X.C., Song, W.H., Wang, K.Y., Hu, T., Zhao, B. Sun, Y.P. and Du, J.J., (2001). Preparation and photoluminescence properties of amorphous silica nanowires, *Chemical Physics Letters*, Vol., 336, pp 53-56, 0009-2614.

Yang, Z.M., Yu, Z., Chen, H., Jiao, Z.F., Jin, Y., He, Y., Gong, M. and Sun, X.S., (2007). Growth of amorphous SiO_2 nanowires on pre-oxidised silicon substrate via CVD, *Journal of Non-Crystalline Solids*, Vol., 354, Issue 15-16, 1731-1735, 0022-3093.

Yao, Y., Li, F.H. and Lee, S.T., (2005). Oriented silicon nanowires on silicon substrates from oxide-assisted growth and gold catalysts, *Chemical Physics Letters*, Vol., 406, 381-385, 0009-2614.

Yu, D.P., Hang, Q.L., Ding, Y., Zhang, H.Z., Bai, Z.G., Wang, J.J., Zou, Y.H., Qian, W., Xiong, G.C. and Feng, S.Q., (1998). Amorphous silica nanowires: Intensive blue light emitter, *Applied Physics Letters*, Vol., 73, 3076-3079, 0003-6951.

Zhang, J., Xu, B.L., Yang, Y.D., Jiang, F.H., Li, J.P., Wang, X.C. and Wang, S.M., (2006). Catalyzed-assisted growth of well-aligned silicon oxide nanowires, *Journal of Non-Crystalline Solids*, Vol., 352, Issues 26-27, pp 2859-2862, 0022-3093.

Zhang, M., Bando, Y., Wada, K. and Kurashima, K., (1999). Synthesis of nanotubes and nanowires of silicon oxide, *Journal of Materials Science Letters*, Vol., 18, 1911-1913.

Zhang, Y.F., Tang, Y.H., Lam, C., Wang, N., Lee, C.S., Bello, I. and Lee, S.T., (2000). Bulk-quantity Si nanowires synthesized by SiO sublimation, *Journal of Crystal Growth*, Vol., 212, 115-118, 0022-0248.

Nanowires Science and Technology

Edited by Nicoleta Lupu

ISBN 978-953-7619-89-3
Hard cover, 402 pages
Publisher InTech
Published online 01, February, 2010
Published in print edition February, 2010

This book describes nanowires fabrication and their potential applications, both as standing alone or complementing carbon nanotubes and polymers. Understanding the design and working principles of nanowires described here, requires a multidisciplinary background of physics, chemistry, materials science, electrical and optoelectronics engineering, bioengineering, etc. This book is organized in eighteen chapters. In the first chapters, some considerations concerning the preparation of metallic and semiconductor nanowires are presented. Then, combinations of nanowires and carbon nanotubes are described and their properties connected with possible applications. After that, some polymer nanowires single or complementing metallic nanowires are reported. A new family of nanowires, the photoferroelectric ones, is presented in connection with their possible applications in non-volatile memory devices. Finally, some applications of nanowires in Magnetic Resonance Imaging, photoluminescence, light sensing and field-effect transistors are described. The book offers new insights, solutions and ideas for the design of efficient nanowires and applications. While not pretending to be comprehensive, its wide coverage might be appropriate not only for researchers but also for experienced technical professionals.

INTECH
open science | open minds

InTech Europe
University Campus STeP Ri
Slavka Krautzeka 83/A
51000 Rijeka, Croatia
Phone: +385 (51) 770 447
Fax: +385 (51) 686 166
www.intechopen.com

InTech China
Unit 405, Office Block, Hotel Equatorial Shanghai
No.65, Yan An Road (West), Shanghai, 200040, China
中国上海市延安西路65号上海国际贵都大饭店办公楼405单元
Phone: +86-21-62489820
Fax: +86-21-62489821

IntechOpen